Editors' Suggestion

Direct Laser Cooling to Bose-Einstein Condensation in a Dipole Trap

Alban Urvoy,* Zachary Vendeiro,* Joshua Ramette, Albert Adiyatullin, and Vladan Vuletić†
Department of Physics, MIT-Harvard Center for Ultracold Atoms and Research Laboratory of Electronics, Massachusetts Institute of Technology, Cambridge, Massachusetts 02139, USA

(Received 27 February 2019; published 24 May 2019)

We present a method for producing three-dimensional Bose-Einstein condensates using *only* laser cooling. The phase transition to condensation is crossed with 2.5×10^4 ^{87}Rb atoms at a temperature of $T_c = 0.6\ \mu$K after 1.4 s of cooling. Atoms are trapped in a crossed optical dipole trap and cooled using Raman cooling with far-off-resonant optical pumping light to reduce atom loss and heating. The achieved temperatures are well below the effective recoil temperature. We find that during the final cooling stage at atomic densities above 10^{14} cm^{-3}, careful tuning of trap depth and optical-pumping rate is necessary to evade heating and loss mechanisms. The method may enable the fast production of quantum degenerate gases in a variety of systems including fermions.

DOI: 10.1103/PhysRevLett.122.203202

Quantum degenerate gases provide a flexible platform with applications ranging from quantum simulations of many-body interacting systems [1] to precision measurements [2]. The standard technique for achieving quantum degeneracy is laser cooling followed by evaporative cooling [3] in magnetic [4–6] or optical traps [7]. Evaporation is a powerful tool, but its performance depends strongly on atomic collisional properties and it requires removal of most of the initially trapped atoms. Laser cooling gases to degeneracy could alleviate those issues, but it has proven difficult to implement.

The elusiveness of laser cooling to Bose-Einstein condensation (BEC) [4,5] for more than two decades [8–11] can be understood as follows: optical cooling requires spontaneous photon scattering that moves entropy from the atomic system into the light field. Such scattering sets a natural atomic temperature scale T_r associated with the recoil momentum from a single photon of wavelength $2\pi\lambda\!\!\!^{-}$ and an associated atomic thermal de Broglie wavelength $\lambda_{\mathrm{dB}} = \sqrt{2\pi\hbar^2/(mk_BT_r)} \sim \lambda\!\!\!^{-}$. Here $\hbar$ is the reduced Planck constant, m the atomic mass, and k_B the Boltzmann constant. BEC must then be achieved at relatively high critical atomic density $n_c \sim \lambda_{\mathrm{dB}}^{-3} \sim \lambda\!\!\!^{-3}$, where inelastic collisions result in heating and trap loss. In particular, light-induced collisional loss becomes severe when $n \gtrsim \lambda\!\!\!^{-3}$ [12,13].

For strontium atoms, where cooling on a spectrally narrow transition is available, a strongly inhomogeneous trapping potential has been used to cool a lower-density thermal bath while decoupling the emerging condensate from the cooling light [14]. Very recently, based on similar principles to the ones presented here, an array of small, nearly one-dimensional condensates has been prepared using degenerate Raman sideband cooling [11,15,16] of ^{87}Rb atoms in a two-dimensional optical lattice [17].

In this Letter, we demonstrate Raman cooling [9,18–21] of an ensemble of ^{87}Rb atoms into the quantum degenerate regime, without evaporative cooling. Starting with up to 1×10^5 atoms in an optical dipole trap, the transition to BEC is reached with up to 2.5×10^4 atoms within a cooling time of ∼1 s. As discussed in detail below, the essential components of our technique are (i) the use of carefully far-detuned cooling light to reduce atom loss and heating at high atomic densities [12,22,23], (ii) a reduced optical pumping rate during the final stage to avoid heating by photon reabsorption (*festina lente* regime [24–26]), (iii) a final cooling of atoms in the high-energy wings of the thermal velocity distribution to achieve subrecoil cooling, and (iv) careful control of the final trap depth to reduce heating induced by inelastic three-body collisions.

Raman cooling of the optically trapped atoms is a two-step process where kinetic energy is first removed via a stimulated two-photon Raman transition that simultaneously changes the internal atomic state. Subsequently, entropy is removed in an optical pumping process that restores the original atomic state via the spontaneous scattering of a photon [see Figs. 1(c) and 1(d)]. The optical pumping into the state $|5S_{1/2}; F = 2, m_F = -2\rangle$ along the z axis is performed with σ^--polarized light. We reduce light-induced loss by using optical pumping light with large negative detuning $\Delta/(2\pi) = -4.33$ GHz from the $|5S_{1/2}; F = 2\rangle$ to $|5P_{1/2}; F' = 2\rangle$ transition of the D_1 line, choosing a detuning far from molecular resonances [see Figs. 1(b) and 1(c) and Ref. [27]]. The far-detuned σ^--polarized beam and a π-polarized beam of similar detuning which propagates in the x-y plane [see Fig. 1(a)] drive the stimulated Raman transition to the state $|5S_{1/2}; 2, -1\rangle$, simultaneously changing the atomic momentum by the two-photon recoil $\hbar(\Delta\mathbf{k})$ [27]. To cool all three directions,

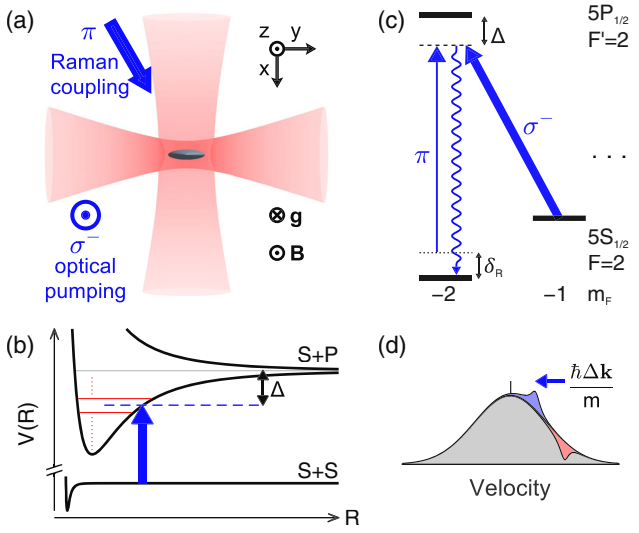

FIG. 1. (a) Geometry of the experimental setup with 795 nm optical pumping and Raman coupling beams, and 1064 nm trapping beams. (b) Molecular potentials. Light-assisted collisions are suppressed if the detuning from atomic resonance Δ is chosen to be far from photoassociation resonances (solid red horizontal lines). (c) Partial atomic level scheme. The Raman transition is resonant for atoms with a two-photon Doppler shift δ_R. (d) Velocity distribution of the atoms along the two-photon momentum $\hbar(\Delta\mathbf{k})$. A Raman transition reduces the velocity of atoms in the velocity class $\delta_R/|\Delta\mathbf{k}|$ by $\hbar(\Delta\mathbf{k})/m$.

we choose $\hbar(\Delta\mathbf{k})$ to have a nonzero projection along any trap eigenaxis.

Cooling is performed in several stages to allow optimization of the cooling as the atomic temperature and density change. Within each stage, the trapping beam powers, optical pumping rate Γ_{sc}, Raman coupling Rabi frequency Ω_R, and Raman resonance detuning δ_R are held constant. The first two cooling stages, S1 and S2, are performed in a single-beam optical dipole trap (SODT), after which the atoms are transferred to a crossed optical dipole trap (XODT), where we perform three more cooling stages [X1 to X3, see Fig. 2(a)]. During each stage, we characterize the cooling performance using time-of-flight absorption imaging, extracting the atom number N and temperature T. (For the final cooling stage close to the BEC threshhold, we exclude the central part of the time-of-flight image from the temperature fit.) We quantify the cooling performance by the classical phase space density $\mathrm{PSD}_c = N[\hbar\bar{\omega}/(k_B T)]^3$, where $\bar{\omega} = (\omega_x\omega_y\omega_z)^{1/3}$ is the geometric mean of the three trapping frequencies. Far from degeneracy, i.e., for a classical gas, PSD_c is equal to $n(0)\lambda_{\mathrm{dB}}^3$, the true PSD at the center of the cloud. The parameters of each stage are optimized to yield the highest PSD_c at the end of the stage [27].

We load 1×10^5 atoms from a magneto-optical trap into the SODT propagating along the y direction with a 10 μm waist [Fig. 1(a)]. After cooling in stage S1 (see Fig. 2), the trap power and vibration frequencies are reduced, thereby

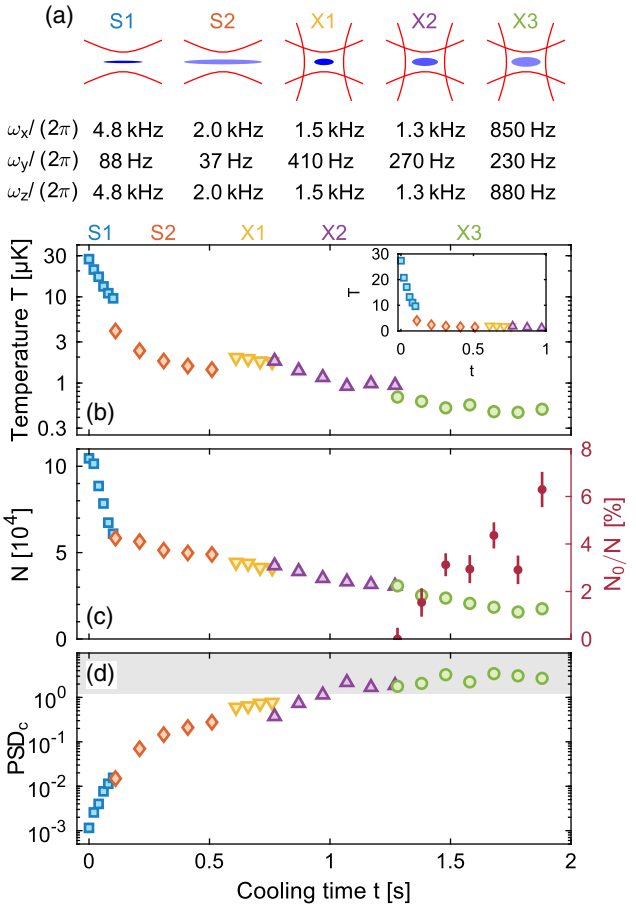

FIG. 2. (a) Schematic of the trapping potential during the cooling sequence, along with the values of the trapping frequencies for each cooling stage. (b) Atomic temperature T as a function of cooling time t. Discrete jumps are caused by changes of the trapping potential between the cooling stages. Inset: Temperature on a linear scale. (c) Atom number (open symbols) and condensate fraction N_0/N (solid circles) during the cooling sequence. (d) Classical phase-space density PSD_c (see main text) as a function of cooling time t. The gray shaded area denotes the quantum degenerate region. Panels (b)–(d) are all plotted along the same time axis.

lowering the density and therefore the loss in stage S2. For all stages, we verify that the trap remains sufficiently deep to keep evaporative cooling negligible.

During stages S1 and S2 we perform fast cooling over 500 ms from 30 μK down to 1.5 μK, and up to PSD_c just below unity. The larger loss rate during S1 relative to the other stages [see Fig. 2(c)] occurs because the Raman cooling cycle, and hence light-induced collision rate, is faster. The initial cooling at high temperatures $T \approx 30$ μK and densities $n < 7 \times 10^{13}$ cm^{-3} is quite efficient, with a logarithmic slope of $\gamma = -d(\ln \mathrm{PSD}_c)/d(\ln N) = 7.2$ [see Fig. 3(a)].

After stage S2 , the ensemble is sufficiently cold so that it can be efficiently transferred in the XODT by ramping up the second trapping beam (18 μm waist, propagating along x)

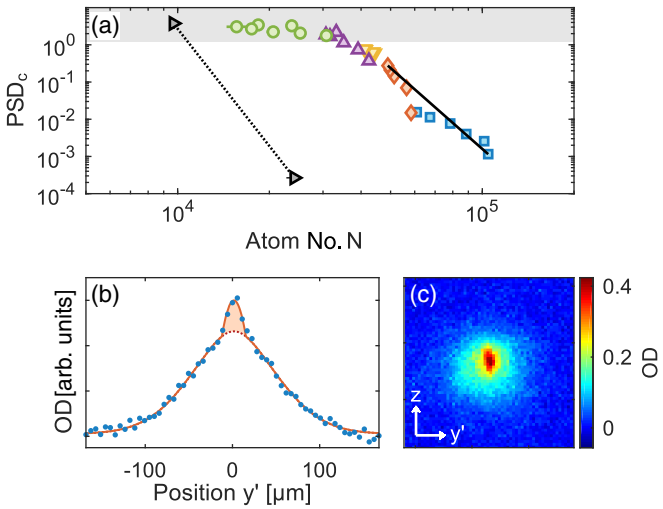

FIG. 3. (a) Classical phase-space density PSD_c as a function of remaining atom number N. The cooling is very efficient until $\mathrm{PSD}_c \sim 1$ is reached. The black symbols denote the performance of the same sequence with the initial atom number reduced by a factor 5. The final atom number is only reduced by a factor 2, indicating a density limit in the cooling. The solid (dashed) black line indicates the S1-S2 (S1-X3) path with an efficiency $\gamma = 7.2$ ($\gamma = 11$) for each case. (b) Line optical density (dots) of the cloud in time of flight along the y' direction (slightly rotated from the y direction in the x-y plane, see Supplemental Material [27]). The data are taken after 1.6 s of cooling and fitted with a $g_{5/2}$ Bose distribution with a Thomas-Fermi distribution superimposed (orange line). The shaded area indicates the condensed fraction. (c) False-color image of the optical density (OD) of the same cloud (before integration along the vertical direction), showing the anisotropic expansion of the condensed fraction in the center.

and applying a short initial cooling (stage X1). In a similar fashion to the S1-S2 sequence, we reduce the confinement of the XODT and cool further during X2, after which the ensemble is at the threshold to condensation. No condensate appears in X2 despite PSD_c reaching the ideal-gas value of 1.2 [33], which we attribute to a combination of the finite size effect [34], the interaction shift [35], and small calibration errors. After further reduction of the XODT, we are able to cross the BEC transition during X3, as shown by the appearance of a condensed fraction in the velocity distribution [see Fig. 3(b)]. The onset of BEC is further confirmed by the anisotropic expansion of the central part of the cloud due to trap confinement anisotropy [see Fig. 3(c)].

In order to achieve BEC, the trap depth during X3 must not be too large. For trap depths much larger than $\sim k_B \times 20\ \mu$K we observe a strong, density-dependent anomalous heating when the Raman cooling is turned off. (Heating rates of up to 10 μK/s are observed at $n \approx 2 \times 10^{14}$ cm^{-3} with a trap depth of $k_B \times 250\ \mu$K.) We surmise that at high atomic densities $n \gtrsim 10^{14}$ cm^{-3}, recombination products of inelastic three-body collisions undergo grazing collisions with trapped atoms, depositing heat in the cloud [27]. This limit on the maximum trap depth is akin to the necessity to maintain, even in the absence of evaporative cooling, a sufficiently low trap depth by applying a so-called "rf shield" in magnetic traps which allows highly energetic nonthermal atoms to escape [36,37].

The BEC transition is crossed with $N \approx 2.5 \times 10^4$ atoms at a critical temperature of $T_c = 0.61(4)\ \mu$K. We are able to reach condensate fractions N_0/N up to 7%. We also verify that if the Raman cooling is turned off during stage X3, the PSD does not increase, and a condensate does not appear. Furthermore, the condensate can be maintained for $\sim$1 s after creation if the cooling is left on, but if the cooling is turned off, the condensate decays within $\sim$100 ms. This confirms that evaporation is insufficient to create or maintain a condensate in this trap configuration, and that the laser cooling is responsible for inducing the phase transition.

For most laser cooling methods, the requisite spontaneous photon scattering sets a recoil temperature limit. Nonetheless, we achieve subrecoil temperatures by addressing atoms in the high-energy wings of the thermal distribution. The optical pumping $|2,-1\rangle \rightarrow |2,-2\rangle$ requires on average the spontaneous scattering of three photons, and therefore imparts $6E_r$ of energy, where $E_r = \hbar^2/(2m\lambda^2) = h \times 3.6$ kHz is the recoil energy of a 795 nm photon. As a result, only atoms with $K_{\Delta\mathbf{k}}/h \gtrsim 29$ kHz of kinetic energy along the $\Delta\mathbf{k}$ direction can be cooled at all [27]. This sets an effective recoil temperature $T_r^{\mathrm{eff}} = 2.8\ \mu$K. We achieve cooling below this effective recoil limit down to 0.5 μK, i.e., a mean kinetic energy $\langle K_{\Delta\mathbf{k}}\rangle/h = 5.2$ kHz, by detuning the Raman coupling so that atoms with more than the average kinetic energy are addressed by the cooling light [27]. However, this slows down the cooling for temperatures below T_r^{eff} (stage S2 onwards), while inelastic collisions add an increased heat load at high densities. In X3 when we cross T_c, we find that under optimized cooling the Raman transition removes 15 kHz of kinetic energy, 30% less than the expected $6E_r$ of heating (see Supplemental Material [27]). This could indicate that the cooling is aided by bosonic stimulation into the condensate during the photon scattering process, in a similar fashion to Ref. [38].

The improved performance of our scheme compared to previous Raman cooling results [9,20] is primarily due to the flexibility to perform optical pumping to a dark state at large detuning from atomic resonances by operating on the D_1 line. To identify suitable detunings, we separately characterized light-induced losses over a 16 GHz frequency range to the red of the bare atomic transition, as shown in Fig. 4(a), and further detailed in the Supplemental Material [27]. Figure 4(b) displays the final atom number and condensate fraction of the optimized sequence as a function of detuning around the value of -4.33 GHz chosen for the experiment. We find that a suitable detuning has to be maintained within ± 50 MHz to ensure good cooling performance.

Another parameter that needs to be optimized is the photon scattering rate Γ_{sc} for optical pumping into the

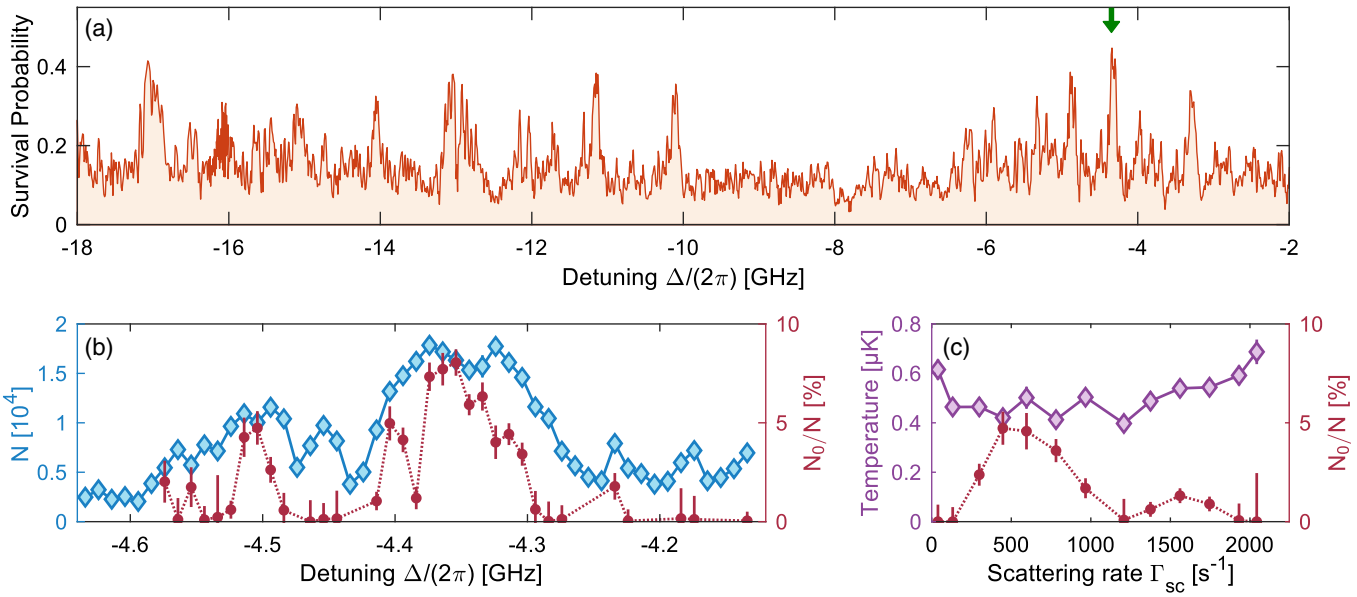

FIG. 4. (a) Photoassociation loss spectrum. Survival probability of trapped atoms as a function of the detuning Δ of the optical pumping beam, when scattering ~100 photons. In substantial portions of the spectrum, the atomic loss is large, due to photoassociation resonances, whereas the peaks correspond to gaps in the photoassociation spectrum away from resonances. The green arrow indicates the detuning used for the data in Figs. 2 and 3. (b) Performance of the full cooling sequence as a function of optical pumping detuning Δ near a locally optimal detuning. A condensate fraction N_0/N is visible only when the losses are limited. To keep the Raman resonance detuning δ_R constant between data points, the magnetic field is adjusted to compensate the change in light shift associated with varying Δ. (c) Temperature and condensate fraction as a function of the scattering rate Γ_{sc} in the final cooling stage. Here, the intensity of the π-polarized beam is adjusted to keep the Raman coupling strength constant between data points, and δ_R is adjusted to optimize the cooling performance for each data point.

$|2,-2\rangle$ dark state. Despite the large detuning, the reabsorption of spontaneously scattered optical pumping photons by other atoms is a resonant two-photon process that can lead to excess heating. However, it was shown theoretically [24,25], and confirmed experimentally [39], that the excess heating can be suppressed at sufficiently low scattering rate Γ_{sc}, such that the confinement and two-photon Doppler broadening reduce the reabsorption probability. This limit is known as the *festina lente* regime. The degradation of the performance at larger Γ_{sc} in Fig. 4(c) is consistent with increased rescattering, as the calculated reabsorption probability approaches unity [27]. A too small value of Γ_{sc}, on the other hand, leads to higher temperatures as parasitic heating mechanisms cannot be compensated when the cooling is too slow.

While ^{87}Rb has relatively favorable collision properties (low two-body inelastic loss rate coefficient and moderate three-body loss rate coefficient in the upper hyperfine manifold), these properties are not unique, and other atomic species may also be suitable for direct laser cooling to BEC. Since the cooling is not *deeply* subrecoil, relatively high densities $n \sim \lambda\!\!\!^{-3}$ are required for reaching BEC. Thanks to the fast cooling, the effect of inelastic loss is small enough if a cloud is stable at these densities (typical lifetime $\gtrsim$1 s at 10^{14} cm^{-3}). Inelastic processes can be further reduced in an effectively one-dimensional geometry [17], where fermionization of the bosonic wave function reduces collisional processes. The demonstrated technique could also be directly applied to fermionic atoms [6], as well as to laser cooled molecules [40,41].

In conclusion, we have realized the decades-old goal of BEC purely by laser cooling by creating a single, moderately sized Bose-Einstein condensate in a standard crossed optical dipole trap. Notably, the method is consistent with the general theoretical recipe put forward by Santos *et al.* [26]. Further work is needed to explore the limits of this new technique in terms of speed, condensate size, and final temperature. [We observe that the performance is still density limited, see Fig. 3(a), and verified that when allowing for moderate final evaporation, nearly pure condensates can be created within a cooling time of 1 s.] It may also be interesting to investigate if this technique can be used to experimentally realize an atom laser, where the condensate is created by bosonic stimulation into the atomic final state during the spontaneous photon scattering [42,43], rather than through thermalizing elastic collisions.

We would like to thank Cheng Chin, Wolfgang Ketterle, and Martin Zwierlein for stimulating discussions and insightful comments. A. A. acknowledges support from the SNSF Grant No. P2ELP2-181926. This work was supported by the NSF, NSF Center for Ultracold Atoms (CUA), NASA, and MURI through ONR.

*These authors contributed equally to this work.
†vuletic@mit.edu

[1] I. Bloch, J. Dalibard, and S. Nascimbène, Quantum simulations with ultracold quantum gases, Nat. Phys. **8**, 267 (2012).
[2] D. Becker *et al.*, Space-borne Bose-Einstein condensation for precision interferometry, Nature (London) **562**, 391 (2018).
[3] W. Ketterle and N. V. Druten, Evaporative cooling of trapped atoms, Adv. At. Mol. Opt. Phys. **37**, 181 (1996).
[4] M. H. Anderson, J. R. Ensher, M. R. Matthews, C. E. Wieman, and E. A. Cornell, Observation of Bose-Einstein condensation in a dilute atomic vapor, Science **269**, 198 (1995).
[5] K. B. Davis, M. O. Mewes, M. R. Andrews, N. J. van Druten, D. S. Durfee, D. M. Kurn, and W. Ketterle, Bose-Einstein Condensation in a Gas of Sodium Atoms, Phys. Rev. Lett. **75**, 3969 (1995).
[6] B. DeMarco and D. S. Jin, Onset of Fermi degeneracy in a trapped atomic gas, Science **285**, 1703 (1999).
[7] M. D. Barrett, J. A. Sauer, and M. S. Chapman, All-Optical Formation of an Atomic Bose-Einstein Condensate, Phys. Rev. Lett. **87**, 010404 (2001).
[8] A. Aspect, E. Arimondo, R. Kaiser, N. Vansteenkiste, and C. Cohen-Tannoudji, Laser Cooling below the One-Photon Recoil Energy by Velocity-Selective Coherent Population Trapping, Phys. Rev. Lett. **61**, 826 (1988).
[9] H. J. Lee, C. S. Adams, M. Kasevich, and S. Chu, Raman Cooling of Atoms in an Optical Dipole Trap, Phys. Rev. Lett. **76**, 2658 (1996).
[10] A. J. Kerman, V. Vuletić, C. Chin, and S. Chu, Beyond Optical Molasses: 3D Raman Sideband Cooling of Atomic Cesium to High Phase-Space Density, Phys. Rev. Lett. **84**, 439 (2000).
[11] D.-J. Han, S. Wolf, S. Oliver, C. McCormick, M. T. DePue, and D. S. Weiss, 3D Raman Sideband Cooling of Cesium Atoms at High Density, Phys. Rev. Lett. **85**, 724 (2000).
[12] K. Burnett, P. S. Julienne, and K.-A. Suominen, Laser-Driven Collisions between Atoms in a Bose-Einstein Condensed Gas, Phys. Rev. Lett. **77**, 1416 (1996).
[13] T. Ido, Y. Isoya, and H. Katori, Optical-dipole trapping of Sr atoms at a high phase-space density, Phys. Rev. A **61**, 061403(R) (2000).
[14] S. Stellmer, B. Pasquiou, R. Grimm, and F. Schreck, Laser Cooling to Quantum Degeneracy, Phys. Rev. Lett. **110**, 263003 (2013).
[15] S. E. Hamann, D. L. Haycock, G. Klose, P. H. Pax, I. H. Deutsch, and P. S. Jessen, Resolved-Sideband Raman Cooling to the Ground State of an Optical Lattice, Phys. Rev. Lett. **80**, 4149 (1998).
[16] V. Vuletić, C. Chin, A. J. Kerman, and S. Chu, Degenerate Raman Sideband Cooling of Trapped Cesium Atoms at Very High Atomic Densities, Phys. Rev. Lett. **81**, 5768 (1998).
[17] J. Hu, A. Urvoy, Z. Vendeiro, V. Crépel, W. Chen, and V. Vuletić, Creation of a Bose-condensed gas of ^{87}Rb by laser cooling, Science **358**, 1078 (2017).
[18] M. Kasevich and S. Chu, Laser Cooling below a Photon Recoil with Three-Level Atoms, Phys. Rev. Lett. **69**, 1741 (1992).
[19] J. Reichel, F. Bardou, M. Ben Dahan, E. Peik, S. Rand, C. Salomon, and C. Cohen-Tannoudji, Raman Cooling of Cesium below 3 nK: New Approach Inspired by Lévy Flight Statistics, Phys. Rev. Lett. **75**, 4575 (1995).
[20] H. Perrin, A. Kuhn, I. Bouchoule, T. Pfau, and C. Salomon, Raman cooling of spin-polarized cesium atoms in a crossed dipole trap, Europhys. Lett. **46**, 141 (1999).
[21] V. Boyer, L. J. Lising, S. L. Rolston, and W. D. Phillips, Deeply subrecoil two-dimensional Raman cooling, Phys. Rev. A **70**, 043405 (2004).
[22] T. W. Hijmans, G. V. Shlyapnikov, and A. L. Burin, Influence of radiative interatomic collisions on dark-state cooling, Phys. Rev. A **54**, 4332 (1996).
[23] J. Rührig, T. Bäuerle, A. Griesmaier, and T. Pfau, High efficiency demagnetization cooling by suppression of light-assisted collisions, Opt. Express **23**, 5596 (2015).
[24] J. I. Cirac, M. Lewenstein, and P. Zoller, Collective laser cooling of trapped atoms, Europhys. Lett. **35**, 647 (1996).
[25] Y. Castin, J. I. Cirac, and M. Lewenstein, Reabsorption of Light by Trapped Atoms, Phys. Rev. Lett. **80**, 5305 (1998).
[26] L. Santos, Z. Idziaszek, J. I. Cirac, and M. Lewenstein, Laser-induced condensation of trapped bosonic gases, J. Phys. B **33**, 4131 (2000).
[27] See Supplemental Material at http://link.aps.org/supplemental/10.1103/PhysRevLett.122.203202, which includes Refs. [9,12,17,18,20,22,24–26,28–32], for details on the optical pumping detuning, the experimental setup, the effective recoil limit, the optimization procedure, and the derivation of the reabsorption probability.
[28] H. Jelassi, B. Viaris de Lesegno, and L. Pruvost, Photoassociation spectroscopy of $^{87}Rb_2$ $(5s_{1/2}+5p_{1/2})$ $0g^-$ long-range molecular states: Analysis by Lu-Fano graph and improved LeRoy-Bernstein formula, Phys. Rev. A **73**, 032501 (2006).
[29] H. Jelassi, B. V. de Lesegno, and L. Pruvost, Photoassociation spectroscopy of $^{87}Rb_2$ $(5s_{1/2}+5p_{1/2})$ $0u^+$ long-range molecular states: Coupling with the $(5s_{1/2}+5p_{3/2})$ $0u^+$ series analyzed using the Lu-Fano approach, Phys. Rev. A **74**, 012510 (2006).
[30] H. Jelassi and L. Pruvost, Weakly bound $^{87}Rb_2$ $(5s_{1/2}+5p_{1/2})$ $1g$ molecules: Hyperfine interaction and LeRoy-Bernstein analysis including linear and nonlinear terms, Phys. Rev. A **89**, 032514 (2014).
[31] J. Schuster, A. Marte, S. Amtage, B. Sang, G. Rempe, and H. C. W. Beijerinck, Avalanches in a Bose-Einstein Condensate, Phys. Rev. Lett. **87**, 170404 (2001).
[32] J. Wolf, M. Deiß, A. Krükow, E. Tiemann, B. P. Ruzic, Y. Wang, J. P. D'Incao, P. S. Julienne, and J. H. Denschlag, State-to-state chemistry for three-body recombination in an ultracold rubidium gas, Science **358**, 921 (2017).
[33] F. Dalfovo, S. Giorgini, L. P. Pitaevskii, and S. Stringari, Theory of Bose-Einstein condensation in trapped gases, Rev. Mod. Phys. **71**, 463 (1999).
[34] W. Ketterle and N. J. van Druten, Bose-Einstein condensation of a finite number of particles trapped in one or three dimensions, Phys. Rev. A **54**, 656 (1996).
[35] R. P. Smith, R. L. D. Campbell, N. Tammuz, and Z. Hadzibabic, Effects of Interactions on the Critical Temperature of a Trapped Bose Gas, Phys. Rev. Lett. **106**, 250403 (2011).

[36] M.-O. Mewes, M. R. Andrews, N. J. van Druten, D. M. Kurn, D. S. Durfee, and W. Ketterle, Bose-Einstein Condensation in a Tightly Confining dc Magnetic Trap, Phys. Rev. Lett. **77**, 416 (1996).
[37] E. A. Burt, R. W. Ghrist, C. J. Myatt, M. J. Holland, E. A. Cornell, and C. E. Wieman, Coherence, Correlations, and Collisions: What One Learns about Bose-Einstein Condensates from Their Decay, Phys. Rev. Lett. **79**, 337 (1997).
[38] N. P. Robins, C. Figl, M. Jeppesen, G. R. Dennis, and J. D. Close, A pumped atom laser, Nat. Phys. **4**, 731 (2008).
[39] S. Wolf, S. J. Oliver, and D. S. Weiss, Suppression of Recoil Heating by an Optical Lattice, Phys. Rev. Lett. **85**, 4249 (2000).
[40] J. F. Barry, D. J. McCarron, E. B. Norrgard, M. H. Steinecker, and D. DeMille, Magneto-optical trapping of a diatomic molecule, Nature (London) **512**, 286 (2014).
[41] L. Anderegg, B. L. Augenbraun, Y. Bao, S. Burchesky, L. W. Cheuk, W. Ketterle, and J. M. Doyle, Laser cooling of optically trapped molecules, Nat. Phys. **14**, 890 (2018).
[42] R. J. C. Spreeuw, T. Pfau, U. Janicke, and M. Wilkens, Laser-like scheme for atomic-matter waves, Europhys. Lett. **32**, 469 (1995).
[43] M. Olshanii, Y. Castin, and J. Dalibard, A model for an atom laser, in *Proceedings of the XII Conference on Laser Spectroscopy*, edited by M. Inguscio, M. Allegrini, and A. Sasso (World Scientific, Singapore, 1996), pp. 7–12.